Kinetic study on HCN volatilization in gold leaching tailing ponds

Izabela Dobrosz-Gómez[a,*], Bayron David Ramos García[b], Edison GilPavas[c],
Miguel Ángel Gómez García[b]

[a] Grupo de Investigación en Procesos Reactivos Intensificados con Separación y Materiales Avanzados – PRISMA, Departamento de Física y Química, Facultad de Ciencias Exactas y Naturales, Universidad Nacional de Colombia, Sede Manizales, Campus La Nubia, km 9 vía al Aeropuerto la Nubia, Apartado Aéreo 127, Manizales, Caldas, Colombia
[b] Grupo de Investigación en Procesos Reactivos Intensificados con Separación y Materiales Avanzados – PRISMA, Departamento de Ingeniería Química, Facultad de Ingeniería y Arquitectura, Universidad Nacional de Colombia, Sede Manizales, Campus La Nubia, km 9 vía al Aeropuerto la Nubia, Apartado Aéreo 127, Manizales, Caldas, Colombia
[c] GIPAB: Grupo de Investigación en Procesos Ambientales, Universidad EAFIT, Carrera 49 #7 sur 50, Medellín, Colombia

ARTICLE INFO

ABSTRACT

In this work, the detailed analysis of HCN volatilization, taking place in tailing storage facilities, was made. Volatilization experiments were performed at conditions typical of gold leaching industrial tailing ponds. The meticulous statistical analysis (including full factorial 3^3 experimental design) let to determine the variables and their interactions affecting the percentage of HCN volatilization. Volatilization tests were performed in an open, temperature-controlled, continuously-stirred batch reactor. The percentage of HCN volatilization was directly proportional to the temperature and temperature-pH interaction and inversely proportional to the pH, cyanide concentration, and pH-pH and temperature-cyanide concentration interactions. HCN volatilization was promoted at acidic conditions. A first order rate law was used to represent the volatilization rate. The specific rate constant (k) was found to be following function of temperature and pH: $k(T,pH) = A_0 \cdot \exp(\frac{-18760.78}{T})$, where: $\ln(A_0) = (0.11 \pm 0.11) \cdot pH + (58.08 \pm 0.16)$. The obtained kinetic model represented properly ($R^2 = 0.90$) experimental data in a wide range of industrial conditions: cyanide concentration (300–2000 mg·L^{-1}), pH (3–9), and temperature (16–20 °C). The increase in temperature, from 16 to 20 °C, let to the increase in k, by a factor of ca. 2.5 ± 0.8. The increase in solution pH, from 3 to 9, provoked its decrease, by a factor of ca. 1.9 ± 0.3.

1. Introduction

The mining industry is one of the most important driving forces in the world's economy. Among a huge variety of ore, gold is one of the most significant mining products. It can be found in minerals, originated from vein material in bedrock deposits, and/or sand or silt grade material in alluvial deposits. The main objective of gold extraction process is to recover the valuable metal from its ore in the purest possible form and with the highest profitability. It can be made by physical (sluice boxes, jigs, shaking tables, spirals, rotating cones, and bowl concentrators) and/or chemical methods (amalgamation and cyanidation) (Chandra and Mubarok, 2016). From chemical ones, cyanidation process, Eq. (1), is preferred, from economic and technical reasons (Parga et al., 2009; Nunan et al., 2017). Moreover, it can be considered as relatively less toxic than amalgamation.

$$4Au + 8NaCN + O_2 + 2H_2O \rightarrow 4Na[Au(CN)_2] + 4NaOH \quad (1)$$

Actually, the cyanidation supports ca. 90% of global gold production (Johnson, 2015). In order to guarantee its high efficiency, solution pH must be alkaline and gold particle size lower than 100 μm (Botz et al., 2016). Since it is not a selective process, cyanide can also react with different metals existing in the mineral, forming their weak complexes and increasing the total amount of sodium cyanide needed for gold recovery (Gönen et al., 2004). Thus, the resulting solution, containing free and metal-complexed cyanide, becomes a highly harmful waste. During 2013, only in the USA, 3 billion liters (i.e., 3×10^9 l) of cyanide-containing wastewater were generated. Consequently, the extraction of gold from low-grade ores by cyanidation resulted in a worldwide emission of ca. 20,000 tons of hydrogen cyanide (HCN) into the atmosphere (Acheampong, 2010).

Various approaches, ranging from natural degradation in tailings impoundment (natural attenuation in surface ponds) to highly sophisticated plant applications, have been developed for cyanide degradation in aqueous solution (Kuyucak and Akcil, 2013; Teixeira et al.,

2013a, 2013b). In many countries, natural degradation in tailings ponds has been the most commonly used treatment method in most mills, including these in e.g. Colombia, for many years. Although it is still widely used for cyanide removal, in the last two decades, several processes including biological, chemical, electrochemical and physical have been developed to either supplement or supplant the natural degradation (Kuyucak and Akcil, 2013). In general, from environmental reasons, conventional chemical detoxification systems are preferred, even if they represent higher operational costs. Nevertheless, for some industrial plants, especially small ones, it is still usual to allow natural cyanide degradation in tailing storage ponds. It results from the combination of different processes (volatilization, photodecomposition, chemical oxidation, microbial-oxidation, chemical precipitation, hydrolysis and precipitation on solids) occurring for prolonged periods.

A number of variables such as: nature of cyanide species (Kuyucak and Akcil, 2013), their concentration (Kuyucak and Akcil, 2013), pH (Johnson, 2015), temperature (Botz and Mudder, 2000; Johnson, 2015), aeration (Botz and Mudder, 2000; Kuyucak and Akcil, 2013), agitation velocity (Johnson, 2015), surface area-to-volume ratio (Botz and Mudder, 2000; Johnson, 2015), as well as pond conditions (e.g., area, depth, turbidity, turbulence, ice cover) (Botz and Mudder, 2000; Kuyucak and Akcil, 2013) can influence the HCN volatilization rate. In general, it occurs naturally, when pH of solution to be volatilized turns into acidic one due to carbon dioxide (CO_2) uptake from the atmosphere and/or addition of acidic rainwater or receiving water. Thus, the drop in pH induces a change in the cyanide/hydrogen cyanide equilibrium, favoring the formation of HCN and its subsequent volatilization as hydrocyanic gas (Kuyucak and Akcil, 2013):

$$CN^- + H^+ \leftrightarrow HCN_{(aq)} \rightarrow HCN_{(g)} \quad (2)$$

Under aerobic conditions, cyanide can be initially converted to cyanate, Eq. (3), in the presence of photochemical (sunlight), bacteriological or mineralogical catalyst. Next, cyanate hydrolysis is possible, Eq. (4), forming bicarbonate and ammonium ions (Kuyucak and Akcil, 2013).

$$CN^- + \frac{1}{2}O_2 + (catalyst) \leftrightarrow OCN^- \quad (3)$$

$$OCN^- + 3H_2O \leftrightarrow HCO_3^- + NH_4^+ + OH^- \quad (4)$$
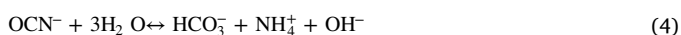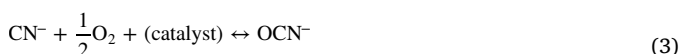
A first order rate law can represent the HCN volatilization rate (Botz and Mudder, 2000):

$$R_{HCN} = k \cdot C_{CN^-} \quad (5)$$

where: k (min^{-1}) is the volatilization rate constant and C_{CN^-} ($mg \cdot L^{-1}$) is the free cyanide concentration (CN^- and HCN).

The range of typical values of HCN volatilization rate constant ($k = (0.07–6.5) \times 10^{-3} min^{-1}$), determined for different surface water bodies (ponds, lakes, rivers), was reported by Kuo and Pilotte (2013). Nevertheless, these values are characteristic of natural water bodies, and can be different for gold industry wastewater. Other authors have also specified the value of k, at bench scale (Dzombak et al., 2006). However, they did not consider that the efficiency of volatilization

process can be affected by the above-mentioned factors (pH, temperature, etc.). Botz et al. (2016) have reported that: (i) k decreases with an increase in solution pH, maintaining air bubbling (1 L·min^{-1}), 48 cm^2 exposed area, and temperature of 20 °C; and (ii) k increases with an increase in cyanide concentration (at 25 °C and pH = 7.9). According to Staunton et al. (2003), k value increases as temperature increases, at fixed pH of 2. Some additional studies have reported on cyanide oxidation at neutral and acid conditions (Wahaab et al., 2010; Shirzad et al., 2011; Farrokhi et al., 2013). However, in these works the cyanide volatilization (as HCN) was roughly mentioned but not quantified.

In order to satisfy new environmental legislation (EPA, 2017) and considering the knowledge available on cyanide chemistry in the liquid phase, more detailed information on its volatilization process is required. Thus, the objective of this research was to gain insight into HCN volatilization kinetics, considering the most crucial parameters (pH, temperature and cyanide concentration) that can affect its efficiency. Here, the Response Surface Methodology (RSM) was applied as a tool to determine the combined effect of processing variables on HCN volatilization efficiency. The RSM is a statistical technique that allows establishing the relationships between several independent variables and one or more dependent ones. It involves the following steps: (i) the implementation of statistically designed experiments; (ii) the estimation of mathematical model coefficients using regression analysis technique; and (iii) the response prediction. Among the available statistical design methods, a factorial 3^3 experimental one was chosen for the purpose of response determination. As far as we know, no similar study was performed on HCN volatilization. Moreover, the sequential experimental analysis was used to develop a kinetic model valid in the following ranges of: (i) pH (3–9), (ii) temperature (16–20 °C), and (iii) cyanide concentration (300–2000 mg·L^{-1}). The volatilization experiments were performed at conditions typical of gold leaching industrial tailing ponds. Subsequently, the volatilization rate constant, as a function of temperature and pH, was adjusted to a semi-theoretical Arrhenius-type expression. It can be considered as a tool to predict HCN volatilization rate from pulp solution in gold-recovery plants.

2. Materials and methods

2.1. Wastewater sample

The cyanide-containing wastewater samples were taken directly from the stream of local gold leaching industrial plant, settled in Caldas Department (Colombia, South America). In order to determine representative cyanide concentration, the sampling was performed quarterly, during one year. For sampling, preservation, storage and transportation, the EPA wastewater-monitoring guide (EPA, 2017) and Standard Methods (APHA, 2012) were taken as references. Table 1 resumes their subsequent, average main characteristics.

Table 1
Summary of average, main characteristics of wastewater coming from the local gold leaching industrial plant.

Parameter	Units	Value	Method	Reference
Temperature	°C	29.4	Mercury-filled thermometer	(APHA, 2012) – SM 2550-Temperature B
pH	–	11.5	Potenciometric	(APHA, 2012) – SM 4500-H^+ B
Conductivity	mS·cm^{-1}	13.2	Conductivimetry	(APHA, 2012) – SM 2510-Conductivity B
Chloride (Cl^-)	mg·L^{-1}	3145	Argentometry	(APHA, 2012) - SM 4500-Cl^- AB
Sulfide (S^{-2})	mg·L^{-1}	102.2	Iodometry	(APHA, 2012) - SM 4500-S^{-2} F
Total cyanide (CN^-)	mg·L^{-1}	300–2000	Distillation-Titration	(APHA, 2012) - SM 4500-CN^- CD

2.2. Reagents

All reagents were used as received, without any further purification. The synthetic aqueous cyanide solutions were prepared using solid potassium cyanide (KCN, Panreac, 97 wt.%) and ultra-pure water (Milli-Q system; conductivity $< 1\mu S\cdot cm^{-1}$). Their pH were measured using a pH-meter Accumet® AB15, equipped with an BOECO-BA-25 electrode, and adjusted with 4 M sodium hydroxide (NaOH, Carloerba, 97 wt.%) or 4 M nitric acid (HNO₃, Merck, 65 wt.%).

2.3. Analytical methods

The titrimetric (4500-CN⁻ D) and colorimetric (4500-CN⁻ E) Standard Methods were implemented to determine and follow cyanide concentration (APHA, 2012). In the titrimetric method, the alkaline distillate from the preliminary treatment (4500-CN⁻ C) was titrated with standard 0.018 M silver nitrate (AgNO₃, Panreac, 99.8 wt.%) to form soluble cyanide complex, $Ag(CN)_2^-$. As soon as all CN⁻ has been complexed and a small excess of Ag⁺ has been added, the excess of Ag⁺ was detected by silver – sensitive indicator, p-dimethylaminobenzalr-hodanine (Across, 99 wt.%), which immediately turned color from yellow to salmon one. If titration showed CN⁻ concentration below $1 \text{ mg}\cdot L^{-1}$, another portion of solution was examined colorimetrically. In the colorimetric method, the alkaline distillate, from preliminary treatment (4500-CN⁻ C), was converted to CNCl by reaction with chloramine-T (Carloerba, analytical grade), at pH < 8 without hydro-lyzing to CNO⁻. As soon as reaction was completed, CNCl formed a red-blue color after the addition of pyridine (Mallinckrodt, 99 wt.%)-barbi-turic acid (Alfa Aesar, 99 wt.%) reagent. The absorbance of the studied solutions was measured at 578 nm wavelength, using a NANOCOLOR® UV/VIS spectrophotometer.

2.4. Experimental set-up

Volatilization experiments were performed in a 250 mL bench scale batch reactor, working at 80% of its capacity, placed permanently in a laminar flow cabinet. Their specific conditions are summarized in Table 2.

The reaction temperature was controlled using a thermostat water bath (Julabo F12-MC) and measured, with the accuracy of ± 0.1 °C, using a thermometer. A stirring plate (Isotemp® 1120049SH) and a magnetic stirrer (2.5 cm) were used to maintain solution homogeneity. Fig. 1 presents the details of experimental set-up. The changes in cyanide concentrations were measured along the time in all experiments. For statistical analysis, the volatilization time was fixed at 1500 min. For kinetics studies, it was varying depending on volatilization conditions.

2.5. Experimental design and statistical analysis

The RSM was implemented to establish the effect of different operating factors (cyanide concentration, temperature and pH) and their interactions on the percentage of HCN volatilization (%Vol). Three different levels (values) were chosen for each of three variables.

Table 2
The experimental conditions for the HCN volatilization tests.

Parameter	Value
Exposed surface area of solution	25 cm²
Solution depth	8 cm
Stirring velocity	200 rpm
UV radiation	No
Metal content	No
Air velocity	Stagnant
Relative humidity	80%
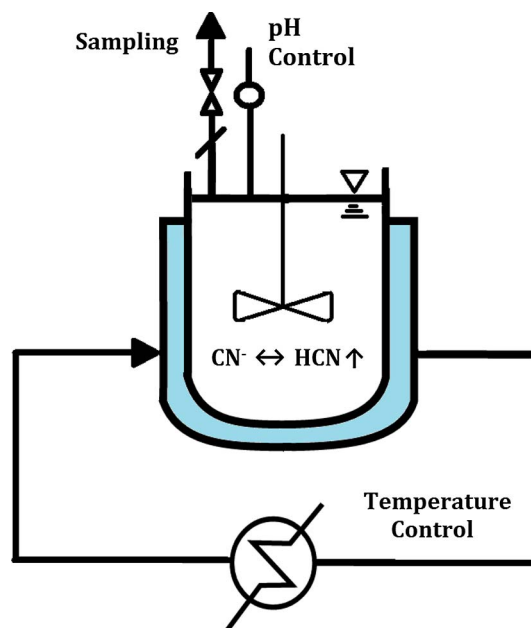
Fig. 1. Schema of the experimental set-up used for the HCN volatilization experiments.

Table 3
The specific conditions of volatilization experiments.

Symbol	Factor	Coded levels		
		−1	0	1
A	Cyanide concentration (mg·L⁻¹)	300	1000	2000
B	Temperature (°C)	16	18	20
C	pH	3	6	9

The range of cyanide concentration was established according to the wastewater sampling results. The analyzed ranges of pH and temperature were similar to these in typical tailing storage facilities. The independent variables and their levels, summarized in Table 3, were coded according to Eq. (6):

$$X_i = \frac{(x_i - x_{pc})}{\Delta x} \tag{6}$$

where: X_i is the coded level, x_i is the uncoded value, x_{pc} corresponds to the uncoded value at the central point, and Δx_i is the change value between (Montgomery, 2009).

The factorial 3^3 experimental design was defined. Thus, 27 experiments, with two replicates each one, were developed. They were programmed using Statgraphics 5.1 (Statistical Graphics Corp 1999–2004) to avoid any systematic error. The temperature, pH, and cyanide concentration were determined after 1500 min of volatilization.

For the RSM, the experimental results were adjusted to a second order multivariable polynomial (Eq. (7)):

$$Yi = \beta_0 + \sum_{i=1}^{3} \beta_i X_i + \sum_{i=1}^{3} \beta_{ii} X_{ii}^2 + \sum_{i=1}^{3} \sum_{j=1}^{3} \beta_{ij} X_i X_j \tag{7}$$

where: Y_i is the predicted response variable; β_0 is the intercept coefficient, β_i is the linear term, β_{ii} is the squared term, and β_{ij} is the interaction term; and X_i and X_j represent the coded independent variables. The quality of this model and its prediction capacity were judged from the variation coefficient, R^2. The significant main and interaction effects of different factors on the percentage of HCN volatilization was followed by analysis of variance (ANOVA). Addition-

ally, the statistical analysis was completed with Pareto diagram and variation coefficients examination.

2.6. Data regression for kinetic study

For kinetic studies, the volatilization experiments were performed under following conditions: initial cyanide concentration = 300, 1000 and 2000 mg·L^{-1}, pH = 3, 6 and 9, temperature = 16, 18 and 20 °C, and time in the range of 0–6000 min., depending on volatilization conditions.

As stated above, a first order rate law, with respect to free cyanide concentration (Eq. (5)) can represent the HCN volatilization rate from aqueous solution (Botz and Mudder, 2000; Dzombak et al., 2006). The combination of Eq. (5) with the mass balance for an isothermal, constant-volume batch reactor makes possible to achieve Eq. (8).

$$\frac{dC_{CN^-}}{dt} = k \cdot C_{CN^-} \tag{8}$$

where k can be obtained from data regression, measuring the cyanide concentration in the solution along the time. Additionally, k depends on other parameters such as temperature and pH. Thus, it can be represented by means of the semi-theoretical relationship of Arrhenius, where the frequency factor A$_0$ is a function of pH (Eqs. (9) and (10)) (Botz et al., 2016).

$$k(T,pH) = A_0 \cdot \exp\left(\frac{-E}{R \cdot T}\right) \tag{9}$$

$$\ln(A_0) = k_1 \cdot pH + k_2 \tag{10}$$

Here, R is the gas constant (8.314 J·K^{-1}·mol^{-1}), T is the absolute temperature (K), E is the volatilization activation energy (J·mol^{-1}), and k$_1$ and k$_2$ are the kinetic parameters.

For data regression, a nonlinear least-squares method "*lsqnonlin*", available in MatLab®, was used. It allows finding A$_0$ and E values that provide the minimum of the objective function (Eq. (11)), which includes the difference between the experimental (k$_e$) and calculated (k) rate constants.

$$f = \sum (k_e - k)^2 = \sum \left(\ln(k_e) - \left(\ln(A_0) - \frac{E}{R \cdot T}\right)\right)^2 \tag{11}$$

3. Results and discussion

3.1. Development of regression model equation

The experimental design together with the obtained data is given in the Supplementary Material (Table S1). The regression analysis was performed to fit the response function (the percentage of HCN volatilization, %Vol). The second order polynomial equation was developed. It represents responses as functions of individual variables, cyanide concentration (A), temperature (B) and pH (C), and their double interactions. An empirical relationship between the response and the input test variables, in coded units, can be expressed as follows:

$$\%Vol = 2.234 \cdot 10^{-2} \cdot A + 15.383 \cdot B - 1.550 \cdot C + 3.610 \cdot 10^{-6} \cdot A^2$$
$$- 1.830 \cdot 10^{-3} \cdot AB - 2.00 \cdot 10^{-4} \cdot AC - 0.245 \cdot B^2 + 0.434 \cdot BC - 0.795 \cdot C^2 \tag{12}$$

Notice that %Vol was linear and quadratic with respect to cyanide concentration, temperature and pH. Moreover, it was linear with respect to the following interactions: cyanide concentration – temperature, cyanide concentration – pH and temperature – pH, indicating that they can also affect volatilization process.

3.2. Analysis of variance (ANOVA)

The analysis of variance, ANOVA, was employed to determine the

Table 4
ANOVA results of the experimental design model.

Factor	Sum of squares	Degree of freedom	Mean square	F ratio	P value
A:Concentration	160.15	1	160.15	11.43	**0.0035**
B:Temperature	3577.73	1	3577.73	255.45	**0.0000**
C:pH	1990.17	1	1990.17	142.10	**0.0000**
AA	40.82	1	40.82	2.91	0.1060
AB	116.19	1	116.19	8.30	**0.0104**
AC	3.14	1	3.14	0.22	0.6418
BB	5.78	1	5.78	0.41	0.5291
BC	81.54	1	81.54	5.82	**0.0274**
CC	307.45	1	307.45	21.95	**0.0002**
Total error	238.10	17	14.01		
Total (corr.)	6521.07	26			

Note: $R^2 = 0.9635$; $R^2_{adj.} = 0.9442$.

significant main and interaction effects of factors influencing the percentage of HCN volatilization, %Vol. The ANOVA results are presented in Table 4.

The ANOVA consists of classifying and cross-classifying statistical results. Fisher *F*-test, defined as the ratio of respective mean-square effect and mean-square error, was used to evaluate the presence of significant difference from control response and to calculate standard errors. The bigger the magnitude of *F* value, more significant the corresponding coefficient is. The *P* values were used to identify experimental parameters that present a statistically significant influence on particular response. If *P* value is lower than 0.05, it is statistically significant with the 95% confidence level (Montgomery, 2009). According to ANOVA results, one can see that not all terms in the regression model are equally important. Only six of them (cyanide concentration (A), temperature (B), pH (C) and their interactions: A-B, B-C and C-C) presented *P* values lower than 0.05 (Table 4). It implies that they present truthfully effect on %Vol, with a confidence interval of 95% (Montgomery, 2009).

The quality of the developed model was evaluated basing on the variation coefficient (R^2) and standard deviation value. The closer R^2 value to unity and lower value of standard deviation, more accurately the model can predict the response. The R^2 value for Eq. (12) was found to be 0.9635, with standard deviation equaled to 3.7420, indicating that 96.35% of the total variation in the percentage of HCN volatilization was attributed to the studied experimental variables. Moreover, the value of predicted R^2 (0.9635) is in very good agreement with the value of adjusted R^2 (0.9442).

3.3. Pareto analysis

The Pareto analysis was used to identify factors that present the greatest cumulative effect on the percentage of HCN volatilization, and to screen out the less significant ones. A Pareto diagram is a series of bars, arranged in descending order of heights from left to right, whose heights reflect the frequency or impact of each factor. Therefore, the factors represented by the tall bars are relatively more significant. Here, the Pareto analysis was also carried out to determine the percentage effect of each factor according to the following equation (Rivera et al., 2014):

$$P_i = \left(\frac{b_i^2}{\sum b_i^2}\right) * 100 (i \neq 0) \tag{13}$$

Thus, statistically important factors correspond to all those which values overpass the inner vertical line (Fig. 2).

This line corresponds to the *t* value in the *t*-student distribution, with a confidence of 95% and for 14 degrees of freedom. Next, this value is compared to the values of each effect and interaction of analyzed factor. The comparison defines the statistical significance of
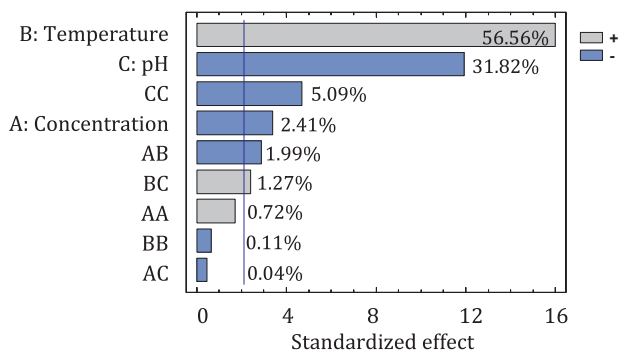
Fig. 2. Pareto diagram for the percentage of HCN volatilization.

each factor in the analyzed process. Therefore, the following factors have an influence on volatilization process: temperature (B), pH (C), cyanide concentration (A) and their following interactions: C-C, A-B, B-C. It could be concluded that the %Vol is directly proportional (+) to the temperature (B) and B-C interaction and inversely proportional (-) to the pH value (C), cyanide concentration (A), C-C and A-B interactions. Notice that temperature and pH can be considered as the most dominating factors during HCN volatilization (Fig. 2). Thus, the kinetic studies focuses on the determination of their effect on the evolution of HCN volatilization with time.

3.4. The kinetic study

3.4.1. The effect of temperature

The effect of temperature on the percentage of HCN volatilization is presented in Fig. 3, as a function of time and pH. Notice that at higher temperature, HCN volatilization is faster. Additionally, at low pH values the percentage of HCN volatilization increases. For example, after 3000 min. test, *ca.* 70% of cyanide was volatilized at pH = 9 and at 16 °C (maximum pH and minimum temperature). On the other hand, at pH = 3 and at 20 °C (minimum pH and maximum temperature), the HCN volatilization was higher than 95%. Additionally, almost complete HCN volatilization ($> 98.8\%$) was detected at 20 °C for cyanide concentration of 300 $mg \cdot L^{-1}$ (specifically at 2000, 2500, and 3000 min. for pH equals to 3, 6, and 9, respectively). At 18 °C, complete HCN volatilization was observed only in a few experiments (*e.g.*, when test time reached 3000 min. and pH was ≤ 6). At 16 °C, complete HCN volatilization was not observed. Such behaviors are in accordance with some data reported in open literature (Dzombak et al., 2006).

Two-film theory, widely accepted for HCN volatilization phenomenon (Chapra, 2008), allows understanding the effect of temperature on volatilization rate. This theory assumes that the following three consecutive steps determine the mass transfer of HCN from the liquid to the gas phase:

1. Mass transfer of HCN through the liquid film.
2. Mass transfer of HCN across the interface.
3. Mass transfer of HCN through the gas film.

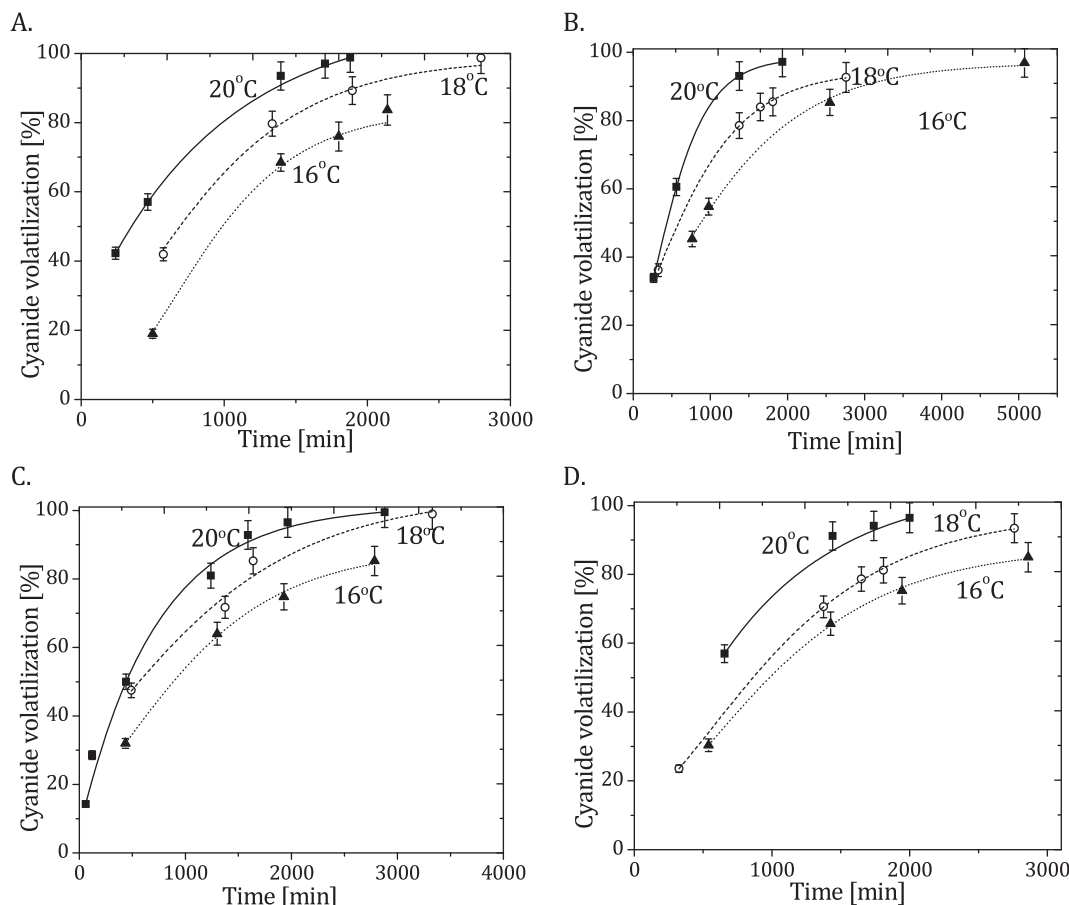In order to define the volatilization rate constant, k, in Eq. (8), as a

Fig. 3. The changes in HCN volatilization percentage vs. time at different temperature. **A**: 300 $mg \cdot L^{-1}$ CN^- and pH 3. **B**: 1000 $mg \cdot L^{-1}$ CN^- and pH 3. **C**: 300 $mg \cdot L^{-1}$ CN^- and pH 6. **D**: 1000 $mg \cdot L^{-1}$ CN^- and pH 6. **E**: 300 $mg \cdot L^{-1}$ CN^- and pH 9. **F**: 1000 $mg \cdot L^{-1}$ CN^- and pH 9. **G**: 2000 $mg \cdot L^{-1}$ CN^- and pH 3. **H**: 2000 $mg \cdot L^{-1}$ CN^- and pH 6. **I**: 2000 $mg \cdot L^{-1}$ CN^- and pH 9.
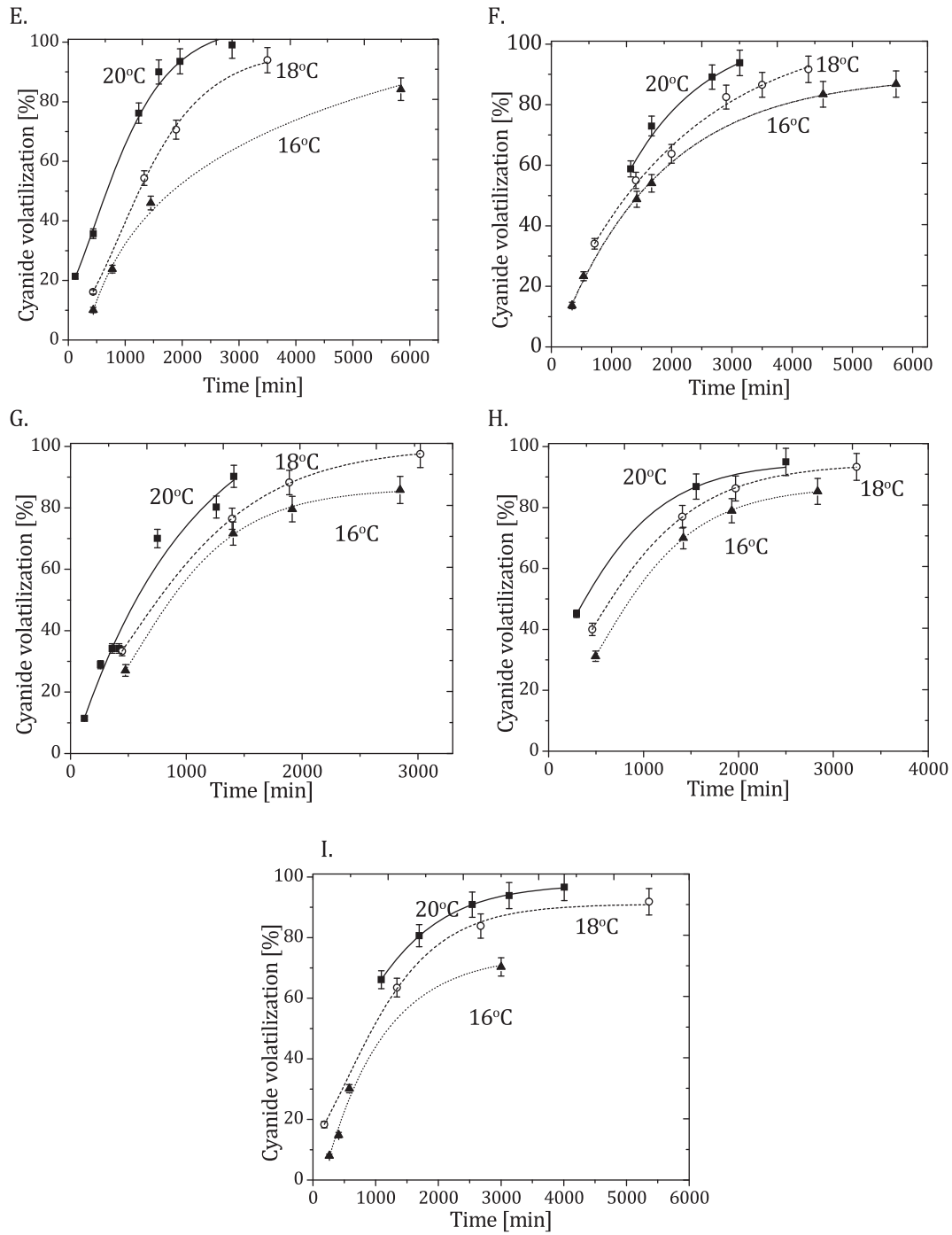
E.

F.

G.

H.

I.

Fig. 3. (*continued*)

function of gas and liquid mass transfer coefficients as well as Henry constant, the following suppositions were made:

(i) Thermodynamic equilibrium reached at gas-liquid interface,
(ii) Negligible concentration gradients in the bulk liquid and gas phases, and
(iii) The mass transfer in steady state, according to the Fick diffusion law (HCN as an ideal gas).

Thus, the volatilization rate constant, k, can be expressed as follows:

$$k = \frac{1}{Z}\left(\frac{1}{k_l} + \frac{R \cdot T}{k_H \cdot k_g}\right)^{-1}$$

(14)

where: Z is the film thickness (cm), k_H is the Henry's law constant (atm·cm³·mol⁻¹), R is the gas constant (atm·cm³·mol⁻¹·K⁻¹), T is the absolute temperature (K) and k_l and k_g are the liquid and gas phase mass transfer coefficients in boundary layer film, respectively (cm·min⁻¹). Notice that k_l, k_g, and k_H parameters, in Eq. (14), are sensitive to the changes in temperature. They increase with an increase in temperature.

3.4.2. The effect of pH

The HCN speciation can be affected by the solution pH through the equilibrium presented in Eq. (2). Thus, the relative concentrations of both HCN and CN^- can be obtained as function of pH, according to the following equation:
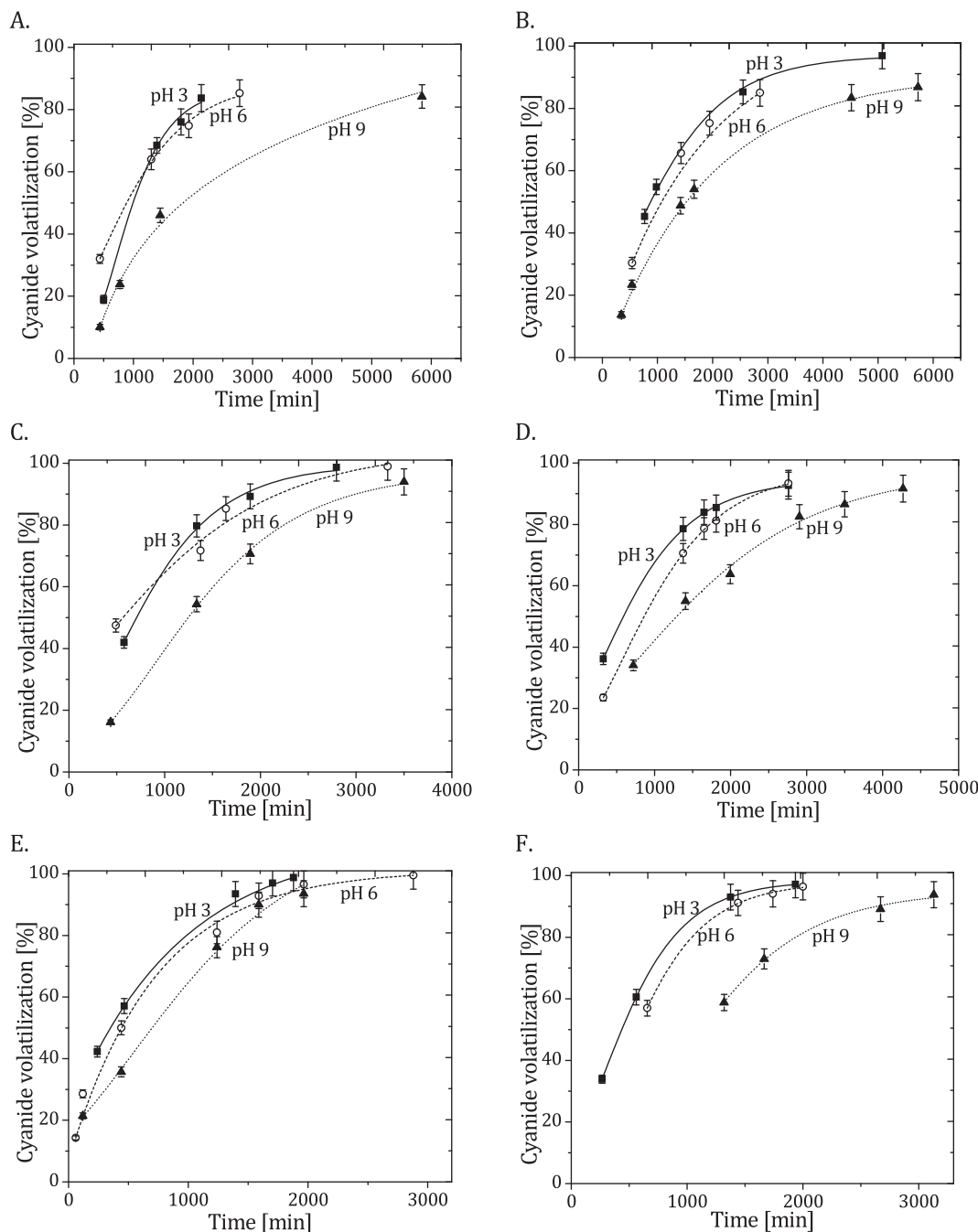
Fig. 4. The changes in HCN volatilization percentage vs. time at different pH values. **A**: 300 mg·L^{-1} CN$^-$ and 16 °C. **B**: 1000 mg·L^{-1} CN$^-$ and 16 °C. **C**: 300 mg·L^{-1} CN$^-$ and 18 °C. **D**: 1000 mg·L^{-1} CN$^-$ and 18 °C. **E**: 300 mg·L^{-1} CN$^-$ and 20 °C. **F**: 1000 mg·L^{-1} CN$^-$ and 20 °C. **G**: 2000 mg·L^{-1} CN$^-$ and 16 °C. **H**: 2000 mg·L^{-1} CN$^-$ and 18 °C. **I**: 2000 mg·L^{-1} CN$^-$ and 20 °C.

$$K_a = \frac{[CN^-][H^+]}{[HCN]} \tag{15}$$

According to the literature (Botz et al., 2016), the pKa value of HCN is 9.3 (at 20 °C and considering negligible ionic strength). Thus, at these conditions, the relative molar concentrations of HCN and CN$^-$ are equivalent. At pH lower than 7, the cyanide mostly exists as molecular one (HCN). Moreover, in the range of pH = 3–6, its relative concentration almost does not change (100–99.95%). The effect of pH on HCN volatilization, at constant conditions of temperature and initial cyanide concentration, is presented in Fig. 4.

HCN volatilization is considerably faster at acidic conditions (pH = 3 and 6). Notice that the course of volatilization curves obtained at pH = 3 and pH = 6 is very similar. It can be attributed to an insignificant difference in relative concentration of HCN in the liquid phase at acidic conditions, as mentioned above. Thus, the concentration gradient of HCN in both phases is invariable and consequently the driving force for its diffusion from liquid to gas phase is almost constant. Similar results have already been reported in the literature for acidification-volatilization experiments carried out at pH = 2.7, at 25 °C, using 358 mg·L^{-1} of cyanide and agitation by air bubbling. These specific conditions let to reach total HCN volatilization (Gönen, 2004).

3.4.3. Data regression

For each experiment, the volatilization rate constant was calculated through the linearization of the solution of Eq. (8). The slope of the curve $Ln\left(\frac{[CN^-]}{[CN^-]_0}\right)$ vs. t allows determining each k value (see
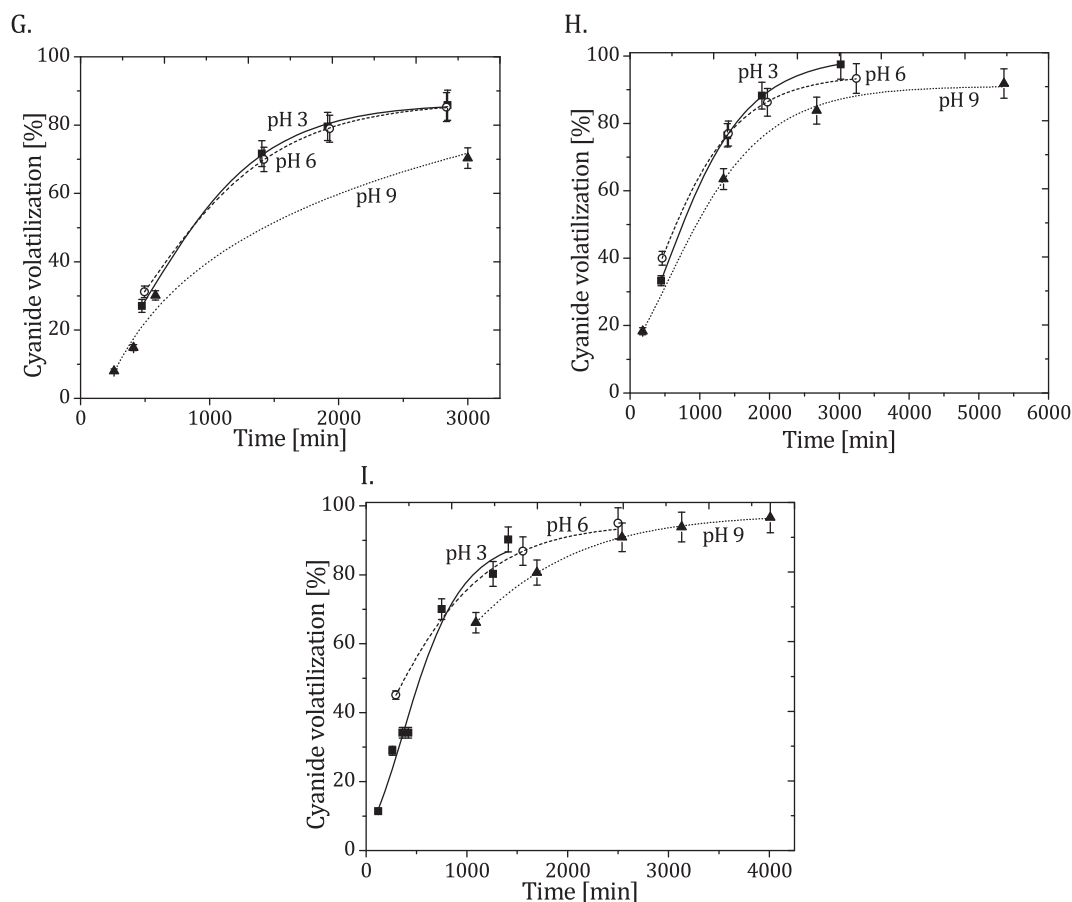
G.

H.

I.

Fig. 4. (*continued*)

Table 5
HCN volatilization rate constants and 95% confidence bounds.

T (°C)	k ($\times 10^{-3}$ min^{-1}) pH		
	3	6	9
300 mg·L^{-1} CN$^-$			
16	0.815 ± 0.093	0.710 ± 0.053	0.322 ± 0.036
18	1.387 ± 0.263	1.284 ± 0.214	0.746 ± 0.124
20	2.157 ± 0.205	1.744 ± 0.143	1.489 ± 0.154
1000 mg·L^{-1} CN$^-$			
16	0.703 ± 0.0470	0.690 ± 0.047	0.380 ± 0.035
18	1.024 ± 0.0936	0.951 ± 0.042	0.576 ± 0.023
20	1.862 ± 0.1005	1.641 ± 0.111	0.839 ± 0.086
2000 mg·L^{-1} CN$^-$			
16	0.754 ± 0.117	0.737 ± 0.100	0.412 ± 0.056
18	1.173 ± 0.101	0.903 ± 0.127	0.523 ± 0.138
20	1.472 ± 0.181	1.234 ± 0.173	0.890 ± 0.054

Table 6
Kinetic parameters, in Eqs. (9) and (10), for cyanide volatilization and 95% confidence bounds.

E$'$R (K)	k$_1$	k$_2$
18760.78	0.11 ± 0.11	58.08 ± 0.16
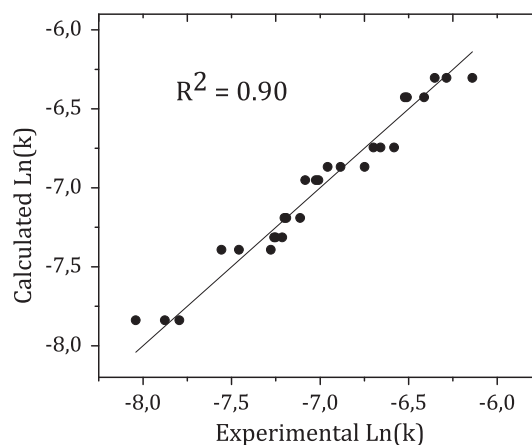
Fig. 5. Parity plot of HCN volatilization rate constant: experimental *vs.* calculated data.

Supplementary Material, Fig. S1). Table 5 resumes k values obtained with data regression, together with their standard deviations (95% confidence bounds). It is evident that volatilization rate was significantly higher in the experiments performed at acidic conditions (pH = 3 and 6). Notice that, for volatilization developed at 16 °C, using 1000 mg·L^{-1} and 2000 mg·L^{-1} of cyanide the obtained values of the fitted slopes are comparable.

The increase in temperature, from 16 to 20 °C, let to the increase in obtained k values, by a factor of *ca.* 2.5 ± 0.8. The effect of cyanide concentration on the obtained k values depended on volatilization temperature. Thus, for HCN volatilization performed at 18 °C and 20 °C, the increase in cyanide concentration, from 300 to 2000 mg·L^{-1},

provoked a decrease in k values. For volatilization at 16 °C, the increase in cyanide concentration from 300 to 1000 mg·L^{-1} also let to the decrease in k. However, the subsequent increase in cyanide concentration to 2000 mg·L^{-1} let to the increase in k. Finally, the increase in solution pH from 3 to 9, provoked the decrease in k, by a factor of *ca.* 1.9 ± 0.3.
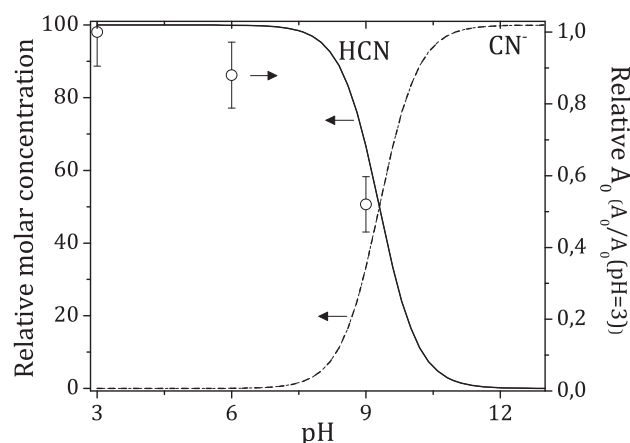
Fig. 6. Relative HCN/CN$^-$ molar concentration and A_0.

Table 7
Comparison of kinetics parameters (k, min^{-1}, and E, kJ·mol^{-1}), at different volatilization conditions, obtained in this study with these reported in open literature.

Volatilization conditions			Kinetic parameters		Reference
C_{CN^-} (mg·L^{-1})	pH	T (°C)	k (× 10^{-3} min^{-1})	E (kJ·mol^{-1})	
20–500	< 7	26	2.15	n.r.	Dzombak et al. (2006)
0.125	7.9	25	0.40	n.r.	Botz et al. (2016)
0.2	7.9	25	0.50	n.r.	
0.26	2	25	5.70	n.r.	Staunton et al. (2003)
0.26	2	35	7.00	n.r.	
0.26	2	40	18.0	n.r.	
2.5	7	20	4.20	70.5	Botz et al. (2016)
2.5	9	20	1.30		
2.5	11	20	0.26		
30	< 3	20	0.07	n.r.	Kuo and Pilotte (2013)
30	< 3	25	6.50	n.r.	
300	3	16	0.82	156	This work
300	9	16	0.32		
300	3	20	2.16		
300	9	20	1.49		
2000	3	16	0.75		
2000	9	16	0.41		
2000	3	20	1.47		
2000	9	20	0.89		

n.r. – not reported.

Once the k values were determined as function of temperature, the kinetic parameters (E/R and A_0) were calculated, using the Arrhenius relationship (Eqs. (9) and (10)), and are presented in Table 6.

To visualize the goodness of the obtained fit, a parity plot was made (Fig. 5). Its R^2 value, close to unity (R^2 = 0.90), shows that this model represents properly 90% of the obtained data and that there is a good agreement between the experimental and predicted data. Thus, the proposed expression of volatilization rate constant, as a function of temperature and pH, can be useful to represent the behavior of HCN volatilization process.

The careful analysis of A_0 changes with pH showed that it decreases with an increase in pH. It can be better understood plotting the relation of $A_0/A_{0(pH=3)}$ *vs.* pH, as presented in Fig. 6. Here, the chemical equilibrium between CN$^-$ and HCN is also included (e.g., the relative HCN and CN$^-$ molar concentration curves were obtained solving Eq. (15) for the pKa value of 9.3). At acidic conditions (pH = 3–6), the free cyanide concentration practically corresponds to HCN. Nevertheless, at pH = 9, the HCN relative concentration decreases to 66.6% (33.4% CN$^-$). Notice that the obtained $A_0/A_{0(pH=3)}$ values follow the tendency of HCN equilibrium curve. Considering that the calculus of equilibrium

curves, plotted in Fig. 6, did not take into account the activity coefficients of all involved species, the slight deviation of experimental points, at pH = 6 and pH = 9, from the equilibrium curves can be understood.

Finally, the comparison of kinetics parameters (k, min^{-1}, and E, kJ.mol^{-1}), at different volatilization conditions, obtained in this study with these reported in open literature is presented in Table 7.

Notice that HCN volatilization rate constant significantly depends on volatilization conditions (temperature, pH and cyanide concentration). In general, (i) k increases with an increase in temperature and cyanide concentration, and (ii) k decreases with an increase in pH. The range of typical values of HCN volatilization rate constant determined in this study ((0.32 < k < 2.16) × 10^{-3} min^{-1}) is within the ranges reported in open literature for either different surface water bodies ((0.07 < k < 6.5) × 10^{-3} min^{-1}) or gold industry wastewater ((k < 18) × 10^{-3} min^{-1}). Similarly, E value obtained in this work (156 kJ mol^{-1}) is comparable to the typical values of activation energy for HCN volatilization process (4.2 < E < 418.4 kJ·mol^{-1}).

4. Conclusions

In this work, the detailed analysis of HCN volatilization, taking place in tailing storage facilities, was made. The volatilization experiments were performed at conditions typical of gold leaching industrial tailing ponds. The meticulous statistical analysis (including full factorial 3^3 experimental design) let to determine the variables and their interactions affecting the percentage of HCN volatilization. It was directly proportional to the temperature and temperature-pH interaction and inversely proportional to the pH, cyanide concentration, and pH-pH and temperature-cyanide concentration interactions. A first order rate law represented volatilization rate. The specific rate constant depended on pH and temperature, by means of semi-theoretical Arrhenius relationship. It represented properly (R^2 = 0.90) the experimental data in a wide range of industrial conditions: cyanide concentration (300–2000 mg·L^{-1}), pH (3–9), and temperature (16–20 °C). The increase in temperature, from 16 to 20 °C, let to the increase in volatilization rate constant, by a factor of *ca.* 2.5 ± 0.8. The increase in solution pH, from 3 to 9, provoked its decrease, by a factor of *ca.* 1.9 ± 0.3. The obtained kinetic parameters and some experimental observations were accurately matched with mass transfer (the two-film model) and thermodynamic (chemical equilibrium) theories. Finally, the proposed expression of volatilization rate constant, as a function of temperature and pH, can be useful to represent the behavior of HCN volatilization in tailing ponds used for the reduction of aqueous cyanide content.

Appendix A. Supplementary material

Supplementary data associated with this article can be found, in the online version, at http://dx.doi.org/10.1016/j.mineng.2017.05.001.

References

Acheampong, M., 2010. Removal of heavy metals and cyanide from gold mine wastewater. J. Chem. Technol. Biotechnol. 85, 590–613. http://dx.doi.org/10.1002/jctb.2358.
APHA, 2012. Standard Methods for the Examination of Water and Wastewater, Washington, DC, 22nd ed. .
Botz, M.M., Mudder, T.I., 2000. Modeling of natural cyanide attenuation in tailings

impoundments. Miner. Metall. Process. 17, 228–233.

Botz, M.M., Mudder, T.I., Akcil, A.U., 2016. Cyanide Treatment: Physical, Chemical, and Biological Processes (and references therein). In: Adams, M.D. (Ed.), Gold Ore Processing: Project Development and Operations, 2nd ed. Elsevier Science, Amsterdam, Netherlands, pp. 619–645. http://dx.doi.org/10.1016/B978-0-444-63658-4.00035-9.

Chandra, Mubarok, M.Z., 2016. On the use of lignin-based biopolymer in improving gold and silver recoveries during cyanidation leaching. Min. Eng. 89, 1–9. http://dx.doi.org/10.1016/j.mineng.2015.12.014.

Chapra, S.C., 2008. Surface Water-Quality Modeling. Waveland Press Inc., Long Grove, Illinois.

Dzombak, D.A., Ghosh, R.S., Young, T.C., 2006. Physical-Chemical Properties and Reactivity of Cyanide in Water and Soil (and references therein). In: Dzombak, D.A., Ghosh, R.S., Wong-Chong, G.M. (Eds.), Cyanide in Water and Soil: Chemistry, Risk, and Management. CRC Press, Taylor & Francis Group, pp. 57–92.

EPA, 2017. Laws and Regulations. https://www.epa.gov/laws-regulations (accessed 03.03.2017).

Farrokhi, M., Yang, J.-K., Lee, S.-M., Shirzad-Siboni, M., 2013. Effect of organic matter on cyanide removal by illuminated titanium dioxide or zinc oxide nanoparticles. J. Environ. Health. Sci. Eng. 11, 23. http://www.ijehse.com/content/11/1/23.

Gönen, N., Kabasakal, O.S., Özdil, G., 2004. Recovery of cyanide in gold leach waste solution by volatilization and absorption. J. Hazard. Mater. 113, 231–236. http://dx.doi.org/10.1016/j.jhazmat.2004.06.029.

Johnson, C.A., 2015. The fate of cyanide in leach wastes at gold mines: an environmental perspective. Appl. Geochemist. 57, 194–205. http://dx.doi.org/10.1016/j.apgeochem.2014.05.023.

Kuo, J.-T., Pilotte, J., 2013. Estimation of Volatilization of Toxics for Multimedia Modeling (and references therein). In: Brutsaert, W., Jirka, G.H. (Eds.), Gas Transfer at Water Surfaces. Springer Science + Business Media, Dordrecht, Netherlands, pp. 589–597. http://dx.doi.org/10.1007/978-94-017-1660-4_54.

Kuyucak, N., Akcil, A., 2013. Cyanide and removal options from effluents in gold mining and metallurgical processes. Min. Eng. 50–51, 13–29. http://dx.doi.org/10.1016/j.

mineng.2013.05.027.

Montgomery, D., 2009. Design and Analysis of Experiments, 7th ed. Wiley and Sons, Hoboken, New Jersey.

Nunan, T.O., Lima Viana, I., Peixoto, G.C., Herbert, E., Verster, D.M., Pereira, J.H., Bonfatti, J.M., Teixeira, L.A.C., 2017. Improvements in gold ore cyanidation by pre-oxidation with hydrogen peroxide. Min. Eng. 108, 67–70. http://dx.doi.org/10.1016/j.mineng.2017.01.006.

Parga, J.R., Vázquez, V., Casillas, H.M., Valenzuela, J.L., 2009. Cyanide detoxification of mining wastewaters with TiO2 nanoparticles and its recovery by electrocoagulation. Chem. Eng. Technol. 32, 1901–1908. http://dx.doi.org/10.1002/ceat.200900177.

Rivera, C.A., Gómez García, M.Á., Dobrosz-Gómez, I., 2014. Adsorptive Removal of Cr (VI) from Aqueous Solution on Hydrous Cerium-Zirconium Oxide, Part I: Process Optimization by Response Surface Methodology. Adsorp. Sci. Technol. 32, 209–226.

Shirzad, M., Samarghandi, M.R., Yang, J.-K., Lee, S.-M., 2011. Photocatalytic removal of cyanide with illuminated TiO2. Water Sci. Technol. 64, 1383–1387. http://dx.doi.org/10.2166/wst.2011.738.

Staunton, W., Wardell-Johnson, G., Lye, P., 2003. Improvement of NPI CyanideEmission Estimation Techniques (Gold Industry) AJ Parker Cooperative Research Centre for Hydrometallurgy for Department of Environment Protection. < http://www.npi.gov.au/system/files/resources/9dbbea8f-b557-edc4-a103-92ecc881d463/files/gold.pdf > (accessed 09.05.2017).

Teixeira, L.A.C., Andia, J.P.M., Yokoyama, L., Araújo, F.V. da F., Sarmiento, C.M., 2013a. Oxidation of cyanide in effluents by Caro's Acid. Min. Eng. 45, 81–87. http://dx.doi.org/10.1016/j.mineng.2013.01.008.

Teixeira, L.A.C., Arellano, M.T.C., Sarmiento, C.M., Yokoyama, L., Araújo, F.V. da F., 2013b. Oxidation of cyanide in water by singlet oxygen generated by the reaction between hydrogen peroxide and hypochlorite. Min. Eng. 50–51 (2013), 57–63. http://dx.doi.org/10.1016/j.mineng.2013.06.007.

Wahaab, R.A., Moawad, A.K., Taleb, E.A., Ibrahim, H.S., El-Nazer, H.A.H., 2010. Combined photocatalytic oxidation and chemical coagulation for cyanide and heavy metals removal from electroplating wastewater. World Appl. Sci. J. 8 (4), 462–469.